

SAR-Probe Calibration System Using Reference Dipole Antenna in Tissue-Equivalent Liquid

Nozomu ISHII^{†,††a}, Member, Yukihiro MIYOTA^{†††}, Ken-ichi SATO^{†††}, Nonmembers, Lira HAMADA^{††}, and Soichi WATANABE^{††}, Members

SUMMARY The probe used in the conventional SAR measurement is usually calibrated in a well filled with tissue-equivalent liquid surrounded by a rectangular waveguide and a matching dielectric window in the frequency range from 800 MHz to 3 GHz. However, below 800 MHz, the waveguides are too large to be used for the calibration. Therefore, we have developed another technique of calibrating the SAR-probe, that is, relating the output voltage of the probe to the field intensity produced by a reference antenna in the tissue-equivalent liquid by using two-antenna method. In this paper, the calibration system using the reference dipole antennas in the liquid at 450 MHz, 900 MHz and 2450 MHz is presented and far-field gain of the reference antenna and calibration factor of the SAR-probe are measured and compared with those obtained by using the conventional waveguide system.

key words: specific absorption rate (SAR), probe, calibration, tissue-equivalent liquid, two-antenna method, gain

1. Introduction

Recently, the bioeffects in human due to the mobile communication devices have been concerned along with the popularization of the devices. Particularly, in compliance testing of mobile phone, in view of radio radiation protection [1], measurement and reporting of the specific absorption rate (SAR) is mandatory in many countries.

The SAR is employed as an evaluation index for the electromagnetic fields in the human body, which is shown in

$$\text{SAR} = \frac{\sigma E^2}{\rho} \quad [\text{W/kg}] \quad (1)$$

where E [V/m] is the electric field strength (RMS), σ [S/m] is the conductivity and ρ [kg/m³] is the density of the media. Compliance testing procedure is described in international standards [2], [3]. Recently, an international standard whose scope is the measurement of body-worn wireless devices was issued [4]. This standard describes the measurement method of SAR used in close proximity to the human body except for the ear. In addition, the frequency range

has been extended from 30 MHz to 6 GHz, whereas the previously issued standard treats in the frequency range from 300 MHz to 3 GHz [3].

In order to carry out accurate measurements, it is important to calibrate the probe used in the SAR measurement system. Therefore, the frequency range of calibration techniques of the measurement devices has to be extended up to the above frequency range. The SAR-probe is usually calibrated using a rectangular waveguide with a matching dielectric window between 800 MHz and 3 GHz [2], [3]. However, using this technique is difficult below 800 MHz, due to its large size of waveguides. In lower frequency range, a thermal transfer technique can be used [2], [3], [5]. The basis of this technique is the correlation between the electromagnetic field intensity to the temperature rise of the tissue-equivalent liquid. However, this technique often requires high radiation power of several tens of watts, in order to obtain sufficient temperature rise.

Therefore, we have been investigating on an alternative method for calibrating the SAR-probe, in order to guarantee the accuracy of the measurement and calibration particularly in lower frequency range. The alternative technique which using known electromagnetic fields produced by a reference antenna is also described in the standards [2], [3], [6]. However, some technical and theoretical consideration should be needed in order to build a practical and reliable calibration system. Particularly, to obtain the gain of the reference antenna in the tissue-equivalent liquid is difficult, because the attenuation of the electric field is quite large due to its relatively high conductivity.

In this paper, we propose the calibration technique of the SAR-probe based on an extension of the Friis transmission formula in the near field region [7], [8], to obtain the gain of the reference antenna. First, the theoretical background of our proposed technique is discussed by introducing some novel concepts which are essential to describe the behavior of the electromagnetic fields in the liquid with relatively high conductivity; an extension of the Friis transmission formula in the near-field zone of the radiator and the near field gain that is an extension of the gain which is normally defined in the far-field zone of the radiator. The near field gain is a key quantity of our calibration technique and it can be approximated by a simple algebraic expression as a function of the distance from the radiator. Also, we point out some error causes in the gain and probe calibration. And, we show an example of constructed calibration system in-

Manuscript received March 5, 2011.

Manuscript revised July 8, 2011.

[†]The author is with the Faculty of Engineering, Niigata University, Niigata-shi, 950-2181 Japan.

^{††}The authors are with the National Institute of Information and Communications Technology, Koganei-shi, 184-8795 Japan.

^{†††}The authors are with the NTT Advanced Technology, Musashino-shi, 182-0012 Japan.

a) E-mail: nishii@eng.niigata-u.ac.jp

DOI: 10.1587/transcom.E95.B.60

cluding the reference dipole antennas and some results of the calibration for the SAR-probe to validate our proposed technique by comparing with the calibration results obtained by the other technique.

2. Principle

The belief procedure of calibrating the SAR-probe is given as follows:

- (A) To determine the gain, G , of the reference antenna in the tissue equivalent liquid using two-antenna method.
- (B) To determine the electric field intensity, $|E|$, at the distance, r , from the reference antenna.
- (C) To determine the calibration factor of the SAR-probe by relating the electric field intensity, $|E|$, to measured output voltage, V_i .

In determining the gain of the reference antenna, we adopt an extended Friis transmission formula in the liquid, which is valid in the near-field zone of the reference antenna. The belief procedure of determining the gain is given as follows:

- (A-1) To find the attenuation and phase constants of the liquid, α and β , by measuring complex permittivity of the liquid with the contact probe method.
- (A-2) Two identical reference antennas are arranged to face each other in the liquid. S_{21} between the two antennas is measured as a function of the distance, r .
- (A-3) The near-field gain obtained above is fitted to its theoretical curve to determine the gain, G .

Ideally, it is preferable to measure S_{21} in the far-field zone of the reference antenna, because the near-field gain converges with the gain in the far-field region. However, the loss in the liquid is too large to measure S_{21} in the far-field zone. Therefore, the gain should be estimated by using S_{21} measured in the near-field zone.

2.1 Gain Calibration

The calibration of the reference antenna is based on the two-antenna method for antenna calibration in free space. As shown in Fig. 1, two reference antennas are located to face each other in the liquid surrounded by a rectangular tank. Then, transmitting and receiving antennas are connected to the ports of the vector network analyzer. If the distance

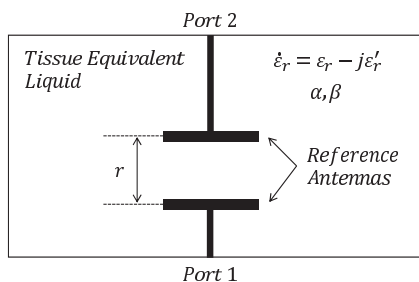


Fig. 1 Gain calibration of the reference antenna operated in the liquid using the modified Friis transmission formula and two-antenna method.

between the two antennas is long enough, the transmitted power can be given as

$$|S_{21}(r)|^2 = (1 - |S_{11}|^2)(1 - |S_{22}|^2) \frac{G_1 G_2 e^{-2\alpha r}}{4\beta^2 r^2}, \quad (2)$$

by making use of the Friis transmission formula which is valid in the far-field zone of the antennas. S_{ij} ($i, j = 1, 2$) are S parameters between the two antennas and $|S_{11}|$ and $|S_{22}|$ are assumed to be independent of the distance, r . Also, G_1 and G_2 are the gains of the transmitting and receiving antennas and should be constant in the far-field zone of the antennas. At the request of the two-antenna method, the condition of $G_1 = G_2 = G_n(r)$ should be applied to Eq. (2). Then, the solution, $G_n(r)$, of Eq. (2) can be given as

$$G_n(r) = \frac{|S_{21}(r)|e^{\alpha r} \cdot 2\beta r}{\sqrt{(1 - |S_{11}|^2)(1 - |S_{22}|^2)}}. \quad (3)$$

We define this $G_n(r)$ as the near-field gain, but it becomes a constant for long distance under the far-field condition. For the large loss in the liquid, S_{21} should be measured in the near-field zone so that the near-field gain, $G_n(r)$, could be treated as a function of the distance, r . Therefore, it is necessary to extend Eq. (2) to be valid in the near-field zone. An extension of Eq. (2) can be given as

$$|S_{21}(r)|^2 = (1 - |S_{11}|^2)(1 - |S_{22}|^2) \frac{G_1 G_2 e^{-2\alpha r}}{4\beta^2 r^2} \times \exp\left(2 \sum_{k=1}^n \frac{c_k}{r^k}\right). \quad (4)$$

In Eq. (4), c_k ($k = 1, 2, \dots, n$) are complex constants which are dependent on the geometry of the antenna as well as the attenuation and phase constants of the liquid. At the request of the two-antenna method, the condition of $G_1 = G_2 = G_f$ should be applied to Eq. (4). Then, the near-field gain, $G_n(r)$ can be given as

$$G_n(r) = \gamma(r)G_f \quad (5)$$

where G_f denotes the gain or the far-field gain of the reference antenna and $\gamma(r)$ is gain reduction factor, which is an extension of Pace's work in free space [9], and can be given as

$$\gamma(r) = \exp\left(\sum_{k=1}^n \frac{C_k}{r^k}\right). \quad (6)$$

The dB representation of Eq. (5) can be expressed as

$$G_{n, \text{dB}}(r) = G_{f, \text{dB}} + \sum_{k=1}^n \frac{C_k}{r^k}. \quad (7)$$

This is a theoretical curve for the dB representation of the near-field gain, $G_{n, \text{dB}}(r)$, where $G_{f, \text{dB}}$ is the dB representation of the gain and C_k ($k = 1, 2, \dots, n$) are real constants. For $n = 2$, Eq. (7) means that $G_{n, \text{dB}}(r)$ consists of $G_{f, \text{dB}}$, the term which is inversely proportional to the distance, r , and

the term which is inversely proportional to the square of the distance, r^2 .

As described above, the dB representation of the gain, $G_{f,\text{dB}}$ can be determined by the following procedure.

- (I) To calculate the near-field gain, $G_n(r_j)$, by substituting measured $S_{21}(r_j)$ at $r = r_j$ to Eq. (3), where $j = 1, 2, \dots, m$.
- (II) To fit the above calculated near-field gain to its theoretical curve (7) and determine the dB representation of the gain, $G_{f,\text{dB}}$, by using the least-square method.

The curve given by Eq. (7) can be also expressed as polynomial equations so that the related curve fitting can reduce to solving simultaneous linear equations with no initial values. Thus, the normal equation in matrix form

$$A\mathbf{x} = \mathbf{b} \quad (8)$$

can be derived. The design matrix A and vectors \mathbf{x} and \mathbf{b} are given as

$$A = \begin{pmatrix} [1] & [r^{-1}] & \cdots & [r^{-n}] \\ [r^{-1}] & [r^{-2}] & \cdots & [r^{-n}] \\ \vdots & \vdots & \ddots & \vdots \\ [r^{-n}] & [r^{-n-1}] & \cdots & [r^{-2n}] \end{pmatrix}, \quad (9)$$

$$\mathbf{x} = \begin{pmatrix} G_{f,\text{dB}} \\ C_1 \\ \vdots \\ C_n \end{pmatrix}, \quad (10)$$

$$\mathbf{b} = \begin{pmatrix} [G_{n,\text{dB}}] \\ [G_{n,\text{dB}} \cdot r^{-1}] \\ \vdots \\ [G_{n,\text{dB}} \cdot r^{-n}] \end{pmatrix}, \quad (11)$$

where $[f] = \sum_{j=1}^m f(r_j)$. The normal equation is known to be often close to singular. In this paper, the normal equation (8) is solved in the manner described in [10], that is, by making use of singular value decomposition. Moreover, it should be noticed that the curve given by Eq. (7) is an asymptotic series expansion of the near-field gain so that ill-behavior of the series can be observed if the fitting range is incorrectly selected.

2.2 Probe Calibration

The electric field intensity radiated by the reference antenna in the far-field zone can be given as

$$|\mathbf{E}(r)|^2 = \frac{30P_{\text{in}}(1 - |\Gamma|^2)G_f}{\text{Re}(\sqrt{\epsilon_r})} \frac{e^{-2\alpha r}}{r^2} \quad (12)$$

where P_{in} is input power, Γ is reflection coefficient of the reference antenna, and ϵ_r is relative complex permittivity of the liquid [3]. In the near-field zone, the decay factor of $e^{-\alpha r}$ should be replaced by $\gamma(r)e^{-\alpha r}$ in Eq. (12). Then, the electric field intensity radiated by the reference antenna in

the near-field zone can be replaced by

$$|\mathbf{E}(r)|^2 = \frac{30P_{\text{in}}(1 - |\Gamma|^2)G_f}{\text{Re}(\sqrt{\epsilon_r})} \frac{\gamma^2(r)e^{-2\alpha r}}{r^2}. \quad (13)$$

In practice, the SAR-probe consists of three orthogonal antennas with Schottky diodes between the elements of the short dipoles on the sides of Δ -shaped tube [2], [3]. According to the square-law operation of the diode, the output voltage of the sensor i , $V_i(r)$, is ideally proportional to the square of the electric field intensity, $|\mathbf{E}_i(r)|^2$ at the location of the sensors, where $i = 0, 1, 2$. Therefore, the total square of the electric field intensity, $|\mathbf{E}(r)|^2$ at the center of the sensors can be obtained by summing up the squares of the electric field intensity, $|\mathbf{E}_i(r)|^2$ for three orthogonal sensors, as follows:

$$|\mathbf{E}(r)|^2 = \sum_{i=0}^2 |\mathbf{E}_i(r)|^2 = \sum_{i=0}^2 \frac{V_i(r)}{K_i(r)}, \quad (14)$$

where $K_i(r)$ is sensitivity factor of the dipole sensor i in the liquid. The actual voltage detected by the sensor i , $U_i(r)$, is affected by diode compression and should be transformed into the ideal sensor voltage $V_i(r)$ in Eq. (14). Also, the sensitivity factor in the liquid, $K_i(r)$, can be decomposed into the sensitivity factor in free space, NF_i , and total sensitivity of the probe in the liquid, $Factor(r)$ as

$$K_i(r) = NF_i \times Factor(r). \quad (15)$$

Then, $Factor(r)$ of the probe can be evaluated by using the voltage V_i at the distance from the reference antenna, r .

3. Error Causes

3.1 Error Causes in Gain Calibration

In the previous section, the attenuation constant is assumed to have no error. However, the uncertainty of the complex permittivity measurement using the contact probe method (Agilent 85070E) is typically 5% for $k = 2$. Therefore, in practice, it is impossible to ignore the uncertainty in the attenuation constant. If the error of the attenuation constant, $\Delta\alpha$, exists, the near-field gain can be reduced as

$$\begin{aligned} G_{n,\alpha+\Delta\alpha}(r) &= C|S_{21}(r)|e^{(\alpha+\Delta\alpha)r} \cdot r \\ &= [C|S_{21}(r)|e^{\alpha r} \cdot r]e^{\Delta\alpha r} = G_{n,\alpha}(r)e^{\Delta\alpha r}, \end{aligned} \quad (16)$$

where $G_{n,\alpha}(r)$ is the near-field gain with the attenuation constant of α and C is a constant which is independent of the distance, r . Then, the dB representation of Eq. (16) can be expressed as

$$G_{n,\alpha+\Delta\alpha,\text{dB}}(r) = G_{n,\alpha,\text{dB}}(r) + 4.343\Delta\alpha r. \quad (17)$$

As the distance, r , is longer, $G_{n,\text{dB}}(r)$ does not converge with $G_{f,\text{dB}}$, but approaches to its asymptotic line, $G_{f,\text{dB}} + 4.343\Delta\alpha r$. For example, if the error of the attenuation constant is given as $\Delta\alpha/\alpha = 5\%$ in the tissue-equivalent liquid

at 2450 MHz, the error of the near-field gain can be estimated as 0.3 dB at the distance of $r = 25$ mm, or, at the middle point of the practical fitting and averaging ranges in our system described later. The way to avoid this error is to accurately measure the relative complex permittivity.

The error of the distance, Δr , can be affected on the near-field gain. In this paragraph, the attenuation constant is assumed to have no error. Then the near-field gain can be approximated as

$$G_n(r + \Delta r) = C|S_{21}(r + \Delta r)|e^{\alpha(r + \Delta r)} \cdot (r + \Delta r) \\ \approx [C|S_{21}(r)|e^{\alpha r} \cdot r]e^{\alpha \Delta r} = G_n(r)e^{\alpha \Delta r}, \quad (18)$$

The dB representation of the above near-field gain can be expressed as

$$G_{n,\text{dB}}(r) \approx G_{n,\text{dB}}(r) + 4.343\alpha\Delta r. \quad (19)$$

It is directly proportional to the error of the distance, Δr . For example, the error of the near-field gain can be estimated as 0.12 dB in the tissue-equivalent liquid at 2450 MHz if the error of the distance is given as $\Delta r = 0.5$ mm, which corresponds to maximum error of the distance practically estimated in our system. This error cannot be ignored if it is hard to determine the center of the reference antenna.

3.2 Error Causes in Probe Calibration

Equations (12) and (13) imply that the sensitivity factor, K_i would be almost proportional to the inverse of the gain, $1/G_f$, and the decay factor, $e^{2\alpha r}$. This means that the fractional error of the sensitivity factor, $\Delta K_i/K_i$, could consist of the fractional error of the gain, $\Delta G_f/G_f$ and the difference of the decay factor, $e^{2\alpha \Delta r} - 1$, if the error of the distance would be given as Δr . For example, $\Delta K_i/K_i = 4.7\%$ if the error of the gain is given as 0.2 dB and $\Delta K_i/K_i = 5.6\%$ if $\Delta r = 0.5$ mm in the liquid at 2450 MHz. Thus, the accurate gain estimation of the reference antenna operated in the liquid and the accurate distance measurement between the reference antenna and the probe are required for the probe calibration.

4. Calibration System

4.1 Reference Antennas

In our calibration system, the dipole antenna is adopted as the reference antenna operated in the tissue-equivalent liquid. The configuration and picture of the reference antennas are shown in Fig. 2, the length of the dipole antennas is listed in Table 1, and the diameter of the dipole rod is 2.4 mm. The length of the reference antennas are determined to be a half of wavelength on the liquid at 450 MHz, 900 MHz and a wavelength in the liquid at 2450 MHz. Also, the antennas are waterproof by covering them with thin rubber. At 2450 MHz, it is difficult to realize a half of wavelength dipole antenna because of waterproof. To reduce the reflection from the antennas, the matching sections with an open

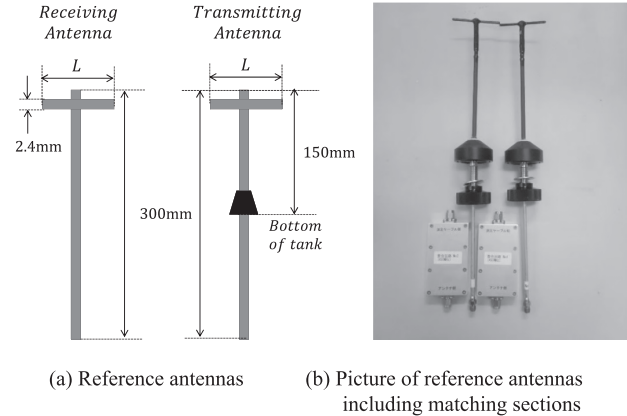


Fig. 2 Reference antenna operated in the liquid and matching sections.

Table 1 Length of the reference antennas and return loss of the reference antennas including matching sections as well as measured dielectric property of the liquid.

Frequency [MHz]	Length [mm]	Return Loss [dB]	Re(ϵ_r)	σ [S/m]
450	50	25.3	44.6	0.89
900	25	41.6	40.4	0.95
2450	19	22.5	38.2	1.83

stub circuit are designed and inserted. Table 1 also lists the return loss of the reference antennas including the matching sections as well as measured dielectric property of the liquid by the contact probe (Agilent 85070E) at three frequencies.

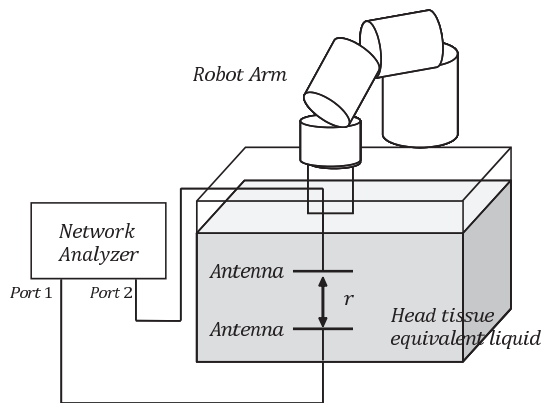
4.2 Gain Calibration

To construct the gain and probe calibration systems, the following conditions should be required as the gain of the reference antenna and calibration factor of the probe are calibrated:

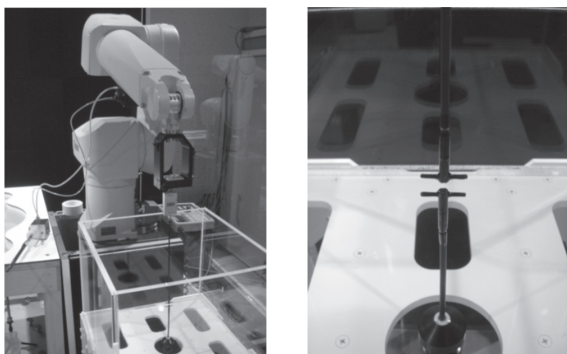
1. The calibration factor of the SAR-probe should be evaluated in the practical way. To evaluate the SAR, the angle between the axis of the probe and surface normal line of the phantom should be smaller than 30° to minimize the boundary effects [3].
2. The output of the SAR-probe should be symmetrical around its axis so that the probe could not be parallel to the direction of the electric field produced by the reference antenna. We found that this axial anisotropy causes the less reproducibility of the measurement results. Also, we should notice that the radiation from the feed cable of the reference antenna is not negligible.

To solve the above difficulties, the transmitting reference antenna is mounted on the bottom of the liquid tank, and the receiving reference antenna and probe are inserted vertically from the top of the tank as shown in Figs. 3 and 4.

In the gain calibration system shown in Fig. 3, the tissue-equivalent liquid is filled to the rectangular tank which has a width of 470 mm, a depth of 470 mm and a height of 390 mm, the transmitting reference antenna is



(a) Schematic overview of proposed gain calibration system



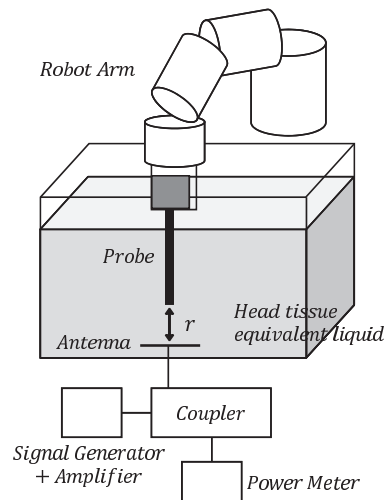
(b) Pictures of gain calibration system and alignment of the antennas

Fig. 3 Gain calibration system for the reference antenna in the liquid.

fixed to a jig in the liquid at a distance of about 150 mm from the bottom of the tank and the receiving reference antenna is moved by the robot arm (Schmid & Partner RX90L). The reference antennas are faced and aligned to match the polarization of the receiving reference antenna to that of the electric field produced by the transmitting reference antenna. They are connected to the vector network analyzer (Agilent 8720ES). Their reflection coefficients and S_{21} between them as a function of their distance is measured as shown in Fig. 3, then the near-field gain can be estimated as a function of the distance by Eq. (3).

4.3 Probe Calibration

In the probe calibration system shown in Fig. 4, the receiving reference antenna in the gain calibration system is replaced with the SAR-probe at the holder of the scanning device. The center of the transmitting reference antenna should be aligned to the sensor of the probe. After measuring the output voltage of the probe by using the power meters (Agilent E4419B/E4418B), sensors (Agilent 8481B) and directional coupler (Agilent 778D) when the transmitting reference antenna produces the fields in the liquid with an arbitrary power level by using the signal generator (Ro-



(a) Schematic overview of proposed probe calibration system



(b) Picture of alignment of the reference antenna and probe

Fig. 4 Probe calibration system.

hde & Schwartz SMIQ03B) and the power amplifier (AR ar_100 W 1000B/MILMEGA AS0408-5L), the calibration factor of the probe can be evaluated by relating the theoretical value of the electric field intensity to the output voltage of the probe.

5. Experimental Results

5.1 Gain Calibration

To determine the initial location of the receiving reference antenna, the transmitting and receiving reference antennas are placed in the liquid at a distance of 8 mm, which is the shortest distance that the antennas have no contact with each other. Then, the distance between the two antennas is changed at an interval of 1 mm to measure S_{21} . Also, S_{11} and S_{22} are also measured at the distance of 20 mm.

The near-field gain of the reference antennas as a function of the distance is plotted as dots at 450 MHz, 900 MHz and 2450 MHz, as shown in Fig. 5. When the distance is over a certain value which depends upon the frequency, the near-field gain is fluctuated due to the reflections from the wall of the tank and the noise caused by the attenuation in

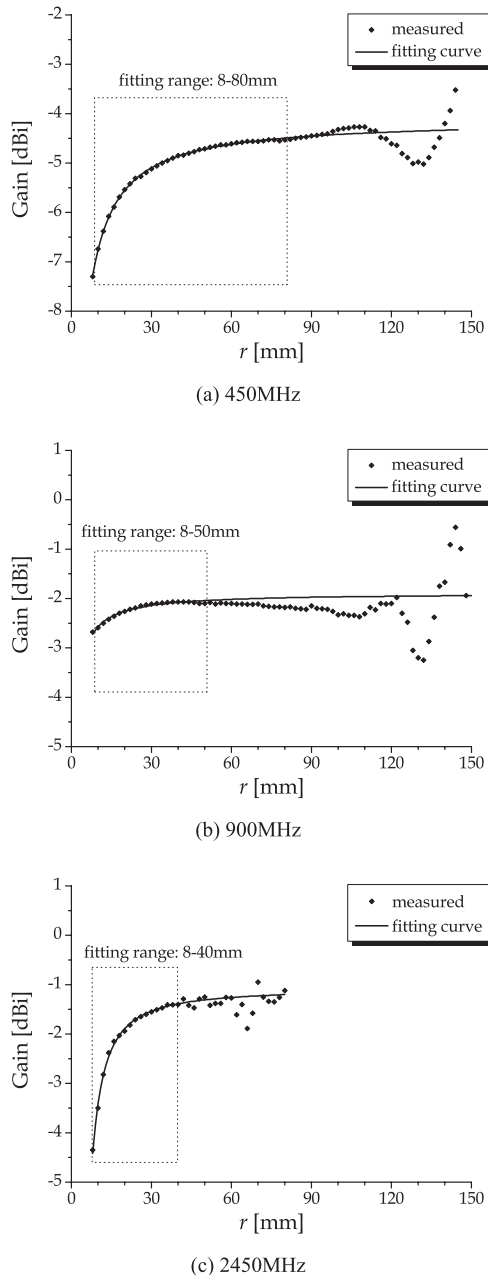


Fig. 5 Measured near-field gain and corresponding fitting curve for $n = 2$ as a function of the distance.

the liquid. Therefore, the fitting range should be carefully selected. That is, the range where the fluctuation can be observed should be excluded from the fitting range.

The fitting range denotes in Figs. 5(a)–(c) at three frequencies. The fitting curve for $n = 2$ is also shown in Fig. 5. The gain and other coefficients in Eq. (7) are listed in Table 2. As shown in Fig. 5, the fitting curve has a good agreement with the measured near-field gain so that the near-field gain can be well approximated by a simple algebraic expression of Eq. (7) in the well-chosen fitting range at three frequencies.

In our formulation, n can be selected as non-negative

Table 2 Calibrated gain in the dB representation, $G_{f,dB}$ and other coefficients, C_k in Eq.(7) of the reference dipole antennas for $n = 2$.

Frequency [MHz]	$G_{f,dB}$ [dBi]	C_1 [dB·mm]	C_2 [dB·mm ²]
450	-4.12	-31.0	46.0
900	-1.89	-7.85	9.91
2450	-1.06	-9.78	-137

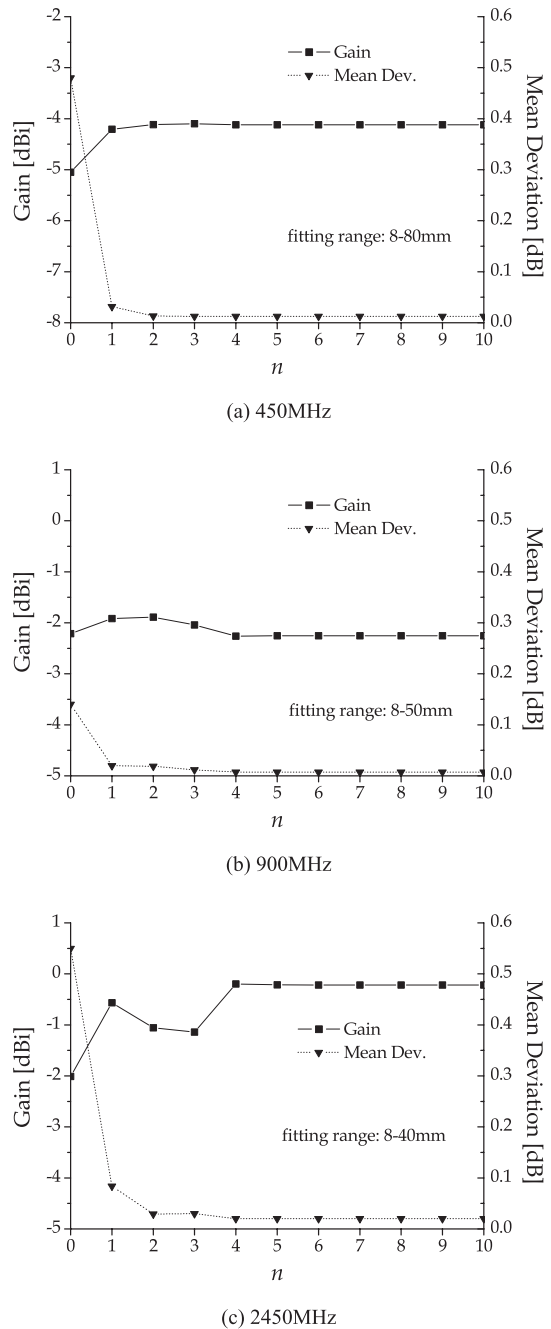


Fig. 6 Gain convergence and mean derivation between measured and estimated near-field gains with the change of n .

integer. Figure 6 shows the gain and its mean derivation between the measured and fitted near-field gains. For $n \geq 4$, the gain and mean derivation are found to be little changed

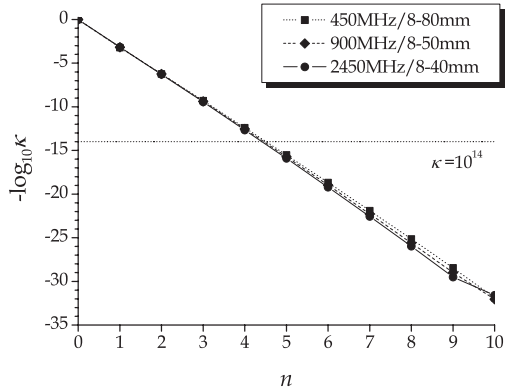


Fig. 7 Condition number of the design matrix, κ , as a function of n .

Table 3 Calibration conditions of the probes.

Frequency [MHz]	Probe* type	Measurement range [mm]	Measurement interval [mm]	Input power [dBm]
450	ET3DV6	8-80	1.0	24
900	ET3DV6	7-80	0.5	24
2450	EX3DV4	6-50	0.5	22

* All probes used in this paper are manufactured by Schmid & Partner Engineering AG.

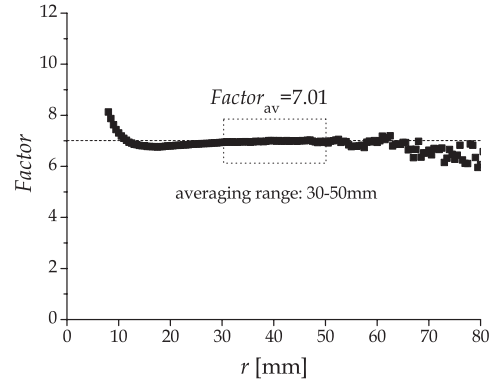
with the increase of n . This is because the condition number of the design matrix in (9), κ , is more than 10^{14} , which corresponds to the inverse of the precision of our calculation, that is, double precision, as shown in Fig. 7. The condition number denotes the measure of the stability for the matrix. In general, when the inverse of the condition number is close to the machine precision, the matrix is said to be ill-conditioned. Therefore, n should be less than 4 in our calculation. Also, the uncertainty of the fitting increases as the number of the unknown coefficients of the normal equation increases [11]. This means that n should be as small as possible, though the error of the gain might be larger. Therefore, we select as $n = 2$ in the above discussion.

5.2 Probe Calibration

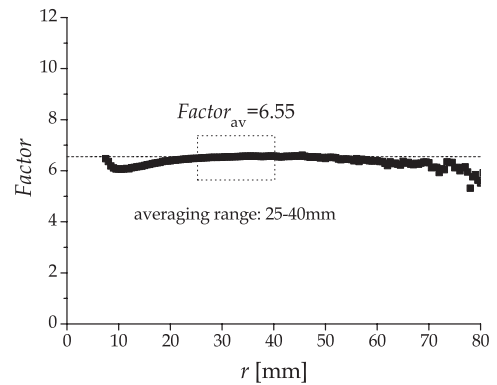
As discussed in 3.1 and 3.2, the error of the distance, Δr , is sensitive to the gain and probe calibration. In our probe calibration, the distance between the reference antenna and the probe is defined as the distance between the center line of the dipole rod of the reference antenna and the center of the probe's sensors. Table 3 lists the measurement range, interval and input power to the reference antenna at three frequencies, 450 MHz, 900 MHz and 2450 MHz.

In our probe calibration, the probe can be calibration at a point by relating the theoretical value of the electric field intensity and the output voltage of the probe. However, $Factor$, defined in (15), is evaluated as a function of the distance, r , to examine the distance property of calibrated $Factor$, experimentally.

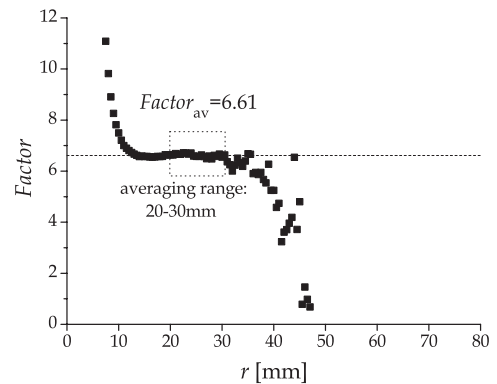
Figure 8 shows the relationship between $Factor$ and the distance, r , at three frequencies, if the near field gain is approximated as Eq. (7) with $n = 2$. To avoid the boundary



(a) 450MHz



(b) 900MHz



(c) 2450MHz

Fig. 8 Plots of $Factor$ as a function of the distance between the reference antenna and the probe at 450 MHz, 900 MHz and 2450 MHz.

and noise effects, $Factor$ should be calibrated in a range of the distance, or averaging range, surrounded by the dotted lines in Fig. 8. Table 4 also lists the averaged $Factor$ in the averaging range, denoted as $Factor_R$, as well as $Factor$ evaluated by the manufacturer's data for the probe calibration [3], denoted as $Factor_W$. The differences of $Factor_R$ from $Factor_W$ are less than 5% or the value of the extended uncertainty of the probe calibration provided by the manufacturer, $U(Factor_W)$, so that the calibrated value of $Factor_R$ could be valid.

Table 4 Comparison between $Factor_R$ and $Factor_W$.

Frequency [MHz]	$Factor_R$	$Factor_W$	Deviation [%]	$U(Factor_W)$ [%] ($k = 2$)
450	7.01	7.16	-2.1	13.3
900	6.55	6.20	5.6	11.0
2450	6.61	6.53	1.2	11.0

6. Conclusions

To develop an alternative method for calibrating the probe used in the standard SAR measurement, we focused on a method of using the reference dipole antennas, based on the extended Friis transmission formula in the liquid and two-antenna method. In this paper, we defined the near-field gain that is an extension of the gain defined in the far-field zone and found the fitting curve that describes the distance property of the near-field gain. Also, the technique of calibrating the SAR-probe by using the fitting curve for the near-field gain. To validate our proposed gain and probe calibrations, we developed the reference dipole antennas operated in the liquid at 450 MHz, 900 MHz and 2450 MHz, and the calibration systems where the reference dipole antenna or probe can be vertically scanned. The calibration results of the SAR-probes obtained by our proposed technique have a good agreement with those obtained by the other calibration technique. Therefore, the proposed calibration for the gain of the reference antenna and the probe can be used instead of the conventional calibrations of the SAR-probe. Assessment of the uncertainty of our method is an issue in the future.

Acknowledgments

This work was partly supported by Grant-in-Aid for Scientific Research from the Japan Society for the Promotion of Science.

References

- [1] International Commission on Non-Ionizing Radiation Protection (ICNIRP), "Guideline on limits of exposure to time-varying electric, magnetic and radiofrequency electromagnetic fields, 1 Hz to 300 GHz," Health Physics, vol.74, pp.495-522, 1998.
- [2] IEEE Standard P1528-2003, "IEEE recommended practice for determining the peak spatial-average specific absorption rate (SAR) in the human head from wireless communications devices: Measurement techniques," IEEE, New York, NY, USA, 2003.
- [3] IEC International Standard 62209-1:2005, "Human exposure to radio frequency fields from hand-held and body-mounted wireless communications devices—Human models, instrumentation, and procedures —, Part 1: Procedure to determine the specific absorption rate (SAR) for hand-held devices used in close proximity to the ear (frequency range of 300 MHz to 3 GHz)," IEC, Geneva, Switzerland, 2005.
- [4] IEC International Standard 62209-2:2010, "Human exposure to radio frequency fields from hand-held and body-mounted wireless communications devices—Human models, instrumentation, and procedures —, Part 2: Procedure to determine the specific absorption rate (SAR) for hand-held devices used in close proximity to the human body (frequency range of 30 MHz to 6 GHz)," IEC, Geneva, Switzerland, 2010.
- [5] L. Hamada, H. Asou, K. Sato, S. Watanabe, and T. Iwasaki, "Development of a SAR-probe calibration system in VHF band based on temperature measurement (2)," Abstracts for the 29th Bioelectromagnetics Society Annual Meeting, P35, pp.313-316, Kanazawa, Japan, June 2007.
- [6] C. Person, L.N. Ahlonsou, and C. Grangeat, "New reference antennas for SAR probe calibration in tissue equivalent liquid," Proc. Millennium Conf. Ant. and Propagat., Abst. #1432, Davos, Switzerland, April 2000.
- [7] N. Ishii, T. Akagawa, K. Sato, L. Hamada, and S. Watanabe, "A method of measuring gain in liquids based on the Friis transmission formula in the near-field region," IEICE Trans. Commun., vol.E90-B, no.9, pp.2401-2407, Sept. 2007.
- [8] N. Ishii, H. Shiga, N. Ikarashi, K. Sato, L. Hamada, and S. Watanabe, "Simultaneous measurement of antenna gain and complex permittivity of liquid in near-field region using weighted regression," IEICE Trans. Commun., vol.E91-B, no.6, pp.1831-1837, June 2008.
- [9] J.R. Pace, "Asymptotic formulas for coupling between two antennas in the Fresnel region," IEEE Trans. Antennas Propag., vol.AP-17, no.3, pp.285-291, May 1969.
- [10] W.H. Press, S.A. Teukolsky, W.T. Vetterlig, and B.P. Flannery, Numerical Recipes, 3rd ed., pp.788-799, Cambridge University Press, New York, 2007.
- [11] N. Ishii, T. Watanabe, Y. Miyota, K. Sato, L. Hamada, and S. Watanabe, "Approximate expression of near field gain in tissue equivalent liquid for SAR evaluation," Proc. 4th International Conference on Electromagnetic Near-Field Characterization and Imaging (ICONIC2009), pp.37-42, Taipei, Taiwan, June 2009.



Nozomu Ishii received the B.S., M.S., and Ph.D. degrees from Hokkaido University, Sapporo, Japan, in 1989, 1991, and 1996, respectively. In 1991, he joined the faculty of Engineering at Hokkaido University. Since 1998, he has been with the faculty of Engineering at Niigata University, Japan, where he is currently an Associate Professor of the Department of the Biocybernetics. His current interests are in the area of small antenna, antenna analysis and measurement. He is a member of the IEEE.



Yukihiko Miyota received the B.E. degree from University of Electro-Communications, Tokyo, Japan in 2000. He joined NTT Advanced Technology Corporation, Tokyo, Japan in 2000. Since 2001, he is working in the field of the electromagnetic compatibility (EMC) problems including biomedical EMC issues, particularly in the Specific Absorption Radio (SAR) measurement.



Ken-ichi Sato received the B.E. and M.E. degrees from Tamagawa University, Tokyo, Japan in 1993 and 1995, respectively. He joined NTT Advanced Technology Corporation, Tokyo, Japan in 1995. From 1999 to 2010, he had worked in the field of the electromagnetic compatibility (EMC) problems including biomedical EMC issues, particularly in the Specific Absorption Radio (SAR) measurement.

Lira Hamada received the Ph.D. degree from Chiba University, Chiba, Japan, in 2000. From 2000 to 2005, she was with the Department of Electronics Engineering, University of Electro-Communications, Chofu, Tokyo, Japan. Since 2005, she has been with the National Institute of Information and Communications Technology (NICT), Koganei, Tokyo, Japan. She is a responsible researcher for the measurement and calibration technique for the SAR evaluation system. Dr. Hamada is a member of the IEE of Japan, the IEEE, and the Bioelectromagnetics Society.



Soichi Watanabe received the B.E., M.E., and D.E., degrees in electrical engineering from Tokyo Metropolitan University, Tokyo, Japan, in 1991, 1993, and 1996, respectively. He is currently with the National Institute of Information and Communications Technology (NICT), Tokyo Japan. His main interest is research on biomedical electromagnetic compatibility. Dr. Watanabe is a member of the Institute of Electrical Engineers (IEE), Japan, the IEEE, and the Bioelectromagnetics Society. He was the recipient of several awards, including the 1996 International Scientific Radio Union (URSI) Young Scientist Award and 1997 Best Paper Award presented by the IEICE.

He was the recipient of several awards, including the 1996 International Scientific Radio Union (URSI) Young Scientist Award and 1997 Best Paper Award presented by the IEICE.